Spectroscopic Methods

International Edition: DOI: 10.1002/anie.201503155
German Edition: DOI: 10.1002/ange.201503155

From Ultrafast Structure Determination to Steering Reactions: Mixed IR/Non-IR Multidimensional Vibrational Spectroscopies

Luuk J. G. W. van Wilderen and Jens Bredenbeck**

Keywords:
2D IR spectroscopy · femtosecond spectroscopy · photochemistry · spectroscopic methods · vibrational spectroscopy

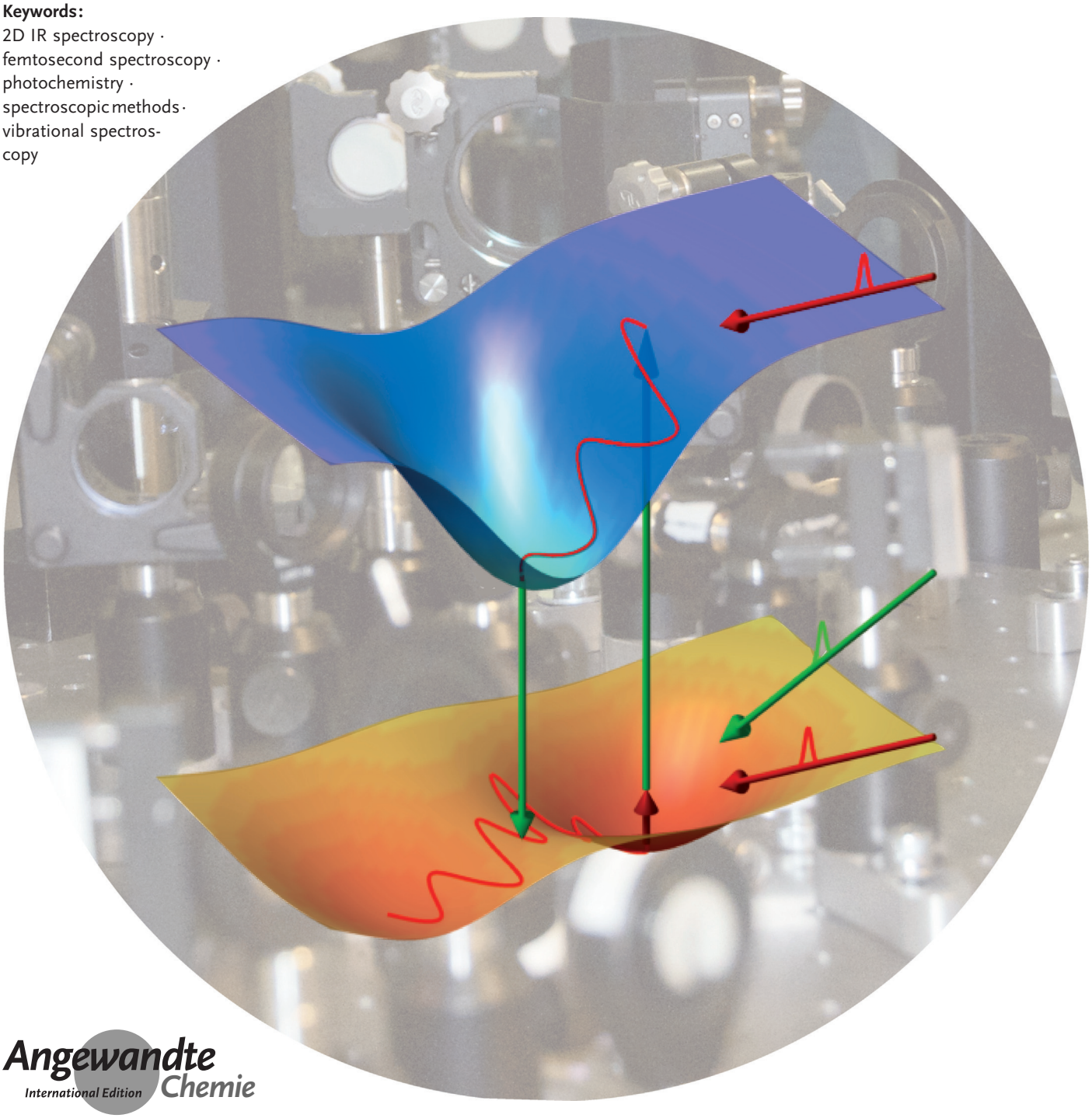

Ultrafast multidimensional infrared spectroscopy is a powerful method for resolving features of molecular structure and dynamics that are difficult or impossible to address with linear spectroscopy. Augmenting the IR pulse sequences by resonant or nonresonant UV, Vis, or NIR pulses considerably extends the range of application and creates techniques with possibilities far beyond a pure multidimensional IR experiment. These include surface-specific 2D-IR spectroscopy with sub-monolayer sensitivity, ultrafast structure determination in non-equilibrium systems, triggered exchange spectroscopy to correlate reactant and product bands, exploring the interplay of electronic and nuclear degrees of freedom, investigation of interactions between Raman- and IR-active modes, imaging with chemical contrast, sub-ensemble-selective photochemistry, and even steering a reaction by selective IR excitation. We give an overview of useful mixed IR/non-IR pulse sequences, discuss their differences, and illustrate their application potential.

From the Contents

1. Introduction 11625

2. A Brief Introduction to 2D-IR Spectroscopy 11626

3. Mixed IR/Non-IR Pulse Sequences 11627

4. Summary and Outlook 11637

1. Introduction

Recent years have witnessed a rapid development of sophisticated techniques that use vibrations in molecules as intrinsic probes to measure structure and dynamics.[1–4] Many aspects make vibrational spectroscopy a very powerful and versatile method. It exhibits high spatial resolution that allows one to follow molecular transformations on the level of functional groups or even single bonds. It offers a high intrinsic time resolution in the sub-picosecond range.[5,6] Vibrations are sensitive to their surroundings, which can modulate their frequency, oscillator strength, and vibrational lifetime. Through these observables, vibrations report on intermolecular interactions, thereby revealing solvation phenomena, hydrogen bonding, or ligand binding. They sense chemical reactions or charge-transfer processes that influence bond strength. They have been used as reporters of local fields inside molecules.[7] As a consequence of anharmonic coupling, they are sensitive to local mechanical energy, thus revealing energy flow.[8] Polarization-sensitive measurements can access the molecular conformation or orientation of certain functional groups.[9,10] IR spectroscopy is compatible with a large variety of samples in the liquid and solid phase, including surfaces and membranes. The high time resolution permits the observation of rapidly interconverting species as separate signal sets in IR absorption spectra. Time-resolved IR spectroscopy down to the sub-picosecond range is widely used to study molecular transformations.

As a result of the wealth of information that can be extracted from vibrational probes, considerable effort has been made to develop multidimensional vibrational spectroscopies, in analogy to multidimensional NMR spectroscopy. These methods use sequences of IR laser pulses to measure couplings and correlations of vibrations with sub-picosecond time resolution, considerably increasing the information content of IR spectroscopy, as detailed in Section 2. They allow, for example, structure determination from the vibrational coupling and the polarization dependence of the signal, the measurement of equilibrium kinetics by exchange spectroscopy, or the investigation of the transfer of vibrational energy, which can be employed, for example, for band assignments.

Augmenting the pure IR pulse sequences with UV, Vis, or NIR (near-IR) pulses dramatically expands the range of applications and possibilities of multidimensional vibrational spectroscopy. The additional pulses can fulfill various purposes. The pure IR experiments are limited to the electronic ground state and usually investigate the system in equilibrium. This excludes many important chemical, physical, and biological processes, which involve electronically excited states or dynamics triggered by electronic excitation. To access such processes, a UV/Vis pulse is required to initiate the dynamic evolution of the system. Furthermore, pulse sequences can be designed to make use of or investigate vibronic coupling. Raman and resonance-Raman processes can be included to provide access to different (polarizability-dependent) observables and create different selectivities, for example, for chromophore modes. Vis or NIR pulses also have been used to upconvert signals from interfaces, thereby enabling interface-specific two-dimensional infrared (2D-IR) spectroscopy with sub-monolayer sensitivity.

As a consequence of ongoing technical developments, such mixed, multidimensional IR-UV/Vis/NIR experiments are becoming more and more accessible. We review various important pulse sequences that have been devised and discuss their differences and application potential to further stimulate their use. The emphasis is on the information content of the experiments, and we have tried to keep technical details and

[*] Dr. L. J. G. W. van Wilderen, Prof. Dr. J. Bredenbeck
Institute of Biophysics, Johann Wolfgang Goethe-University
Frankfurt am Main (Germany)
E-mail: vanwilderen@biophysik.uni-frankfurt.de
bredenbeck@biophysik.uni-frankfurt.de

theoretical background short. We limit ourselves to mixed techniques that feature resonant or nonresonant UV, Vis, or NIR pulses and investigate the coupling or correlation between at least two vibrations, thereby generating a 2D vibrational spectrum. To set the stage, we give a very brief introduction to two-dimensional IR spectroscopy in Section 2 before moving on to the mixed experiments in Section 3.

2. A Brief Introduction to 2D-IR Spectroscopy

2D-IR spectroscopy[11] measures couplings and correlations of vibrational modes to deduce a variety of information on molecular structure and dynamics.[4,12–16] The vibrations do not necessarily need to be in proximity or even on the same molecule. Interpretation of the 2D-IR spectra (see Figure 1) is based on the existence or absence of signals, their shapes, spectral positions, relative sizes, and their evolution in time.

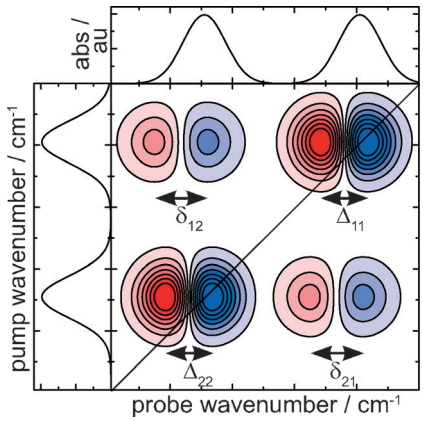

Figure 1. Schematic 2D-IR spectrum of two interacting oscillators. The top and left panels show the linear absorption spectrum of the two oscillators. The 2D-IR panel shows that vibrational excitation of one of the oscillators leads to bleaching and stimulated emission on the diagonal (leading to a negative contribution at the fundamental frequency of the oscillator, in blue) and a concomitant induced absorption (a positive contribution at the first overtone of the oscillator, in red). If the two oscillators interact, off-diagonal peaks (cross-peaks) are generated. The parameters Δ and δ are the observed anharmonic shifts from which diagonal and off-diagonal anharmonicities may be deduced.[4]

To introduce the reader to the field and to set the stage for the discussion of mixed 2D experiments, we focus here on the information content of 2D-IR spectra. The theoretical background and details of the experimental realization of 2D-IR spectroscopy can be found in a number of excellent articles, reviews,[14,15,17–27] and books.[4,16]

2D-IR spectroscopy is a third-order spectroscopy, which means that it uses three resonant interactions of the light field with the sample to induce a signal which is collected by the detector (wavy line in Figure 2). The most straightforward implementation, both technically and for conceiving the idea, is frequency domain *(fd)* 2D-IR spectroscopy (Figure 2A).[11] Here, an intense, narrow-band IR pump pulse (typically a few wavenumbers wide) is scanned across the wavenumber range of interest. Its wavenumber defines the pump axis (see Figure 1 for a schematic spectrum). At a delay t_1 after each pump pulse, a weak broad-band probe pulse measures the change in absorption induced by the pump excitation of the sample. The broad-band probe pulse is dispersed in a spectrometer, which defines the probe axis. The 2D spectrum is thus composed of slices of spectra for the different pump wavenumbers. An alternative implementation is the Fourier transform or time domain (*td*) 2D-IR spectroscopy (pulse sequence in Figure 2B),[28,29] where the narrow-band pump pulse is replaced by a pair of broad-band pulses. The delay τ (the coherence time, see Section 3) between the pulses is scanned and the obtained signal is Fourier transformed with respect to τ to obtain the pump axis of the 2D-IR spectrum. It has been shown that both the *fd* and *td* approaches yield essentially the same information.[30] To illustrate the exchangeability of narrow-band excitation and the use of a pulse pair separated by a delay τ, the corresponding narrow-band pulses in Figure 2 are labeled by a white τ. Whereas the frequency domain approach allows the measurement of selected cuts through 2D spectra and is easier to implement practically, the time domain approach features superior time and wavenumber resolution. For a detailed discussion of these and other experimental realizations and their advantages and disadvantages, the reader is pointed to Ref. [4].

In summary, a 2D-IR spectrum shows the effect of the excitation of a vibrational mode on the other vibrational modes in the spectrum and on the excited mode itself. The excitation and probing of the same vibration gives rise to a so-called diagonal peak. It consists of a negative contribution

Luuk van Wilderen received his PhD at the Vrije Universiteit Amsterdam with Rienk van Grondele and Marie-Louise Groot (2007), after which he joined Jasper van Thor's group at Imperial College London on a FEBS fellowship. He joined Jens Bredenbeck's group at Goethe University Frankfurt in 2010. His main research interests include the development and application of multidimensional spectroscopies, the investigation of the photochemistry of small molecules and proteins, and the development of data analysis methods.

Jens Bredenbeck (born 1975) obtained his Diploma in chemistry in 2000 with R. Schinke (MPI for Flow Research, Göttingen) and his Dr. sc. nat. in 2005 with P. Hamm (Max Born Institute of Nonlinear Optics, Berlin, and University of Zurich). After postdoctoral research with M. Bonn (AMOLF, Amsterdam) he received the Sofja-Kovalevskaja Award of the Humboldt-Foundation and established his group at Goethe University, Frankfurt, in 2007. Since 2010 he has been professor of Experimental Biophysics and Chemical Physics. His research explores molecular structure and dynamics over a wide range of time scales and the development of nonlinear vibrational spectroscopies.

(blue, Figure 1) at the fundamental of the oscillator and a positive contribution of the first overtone, which is anharmonically shifted. Vibrational relaxation leads to a decay of the diagonal peak during time t_1.

Cross-peaks can be generated by various mechanisms and, therefore, can carry different types of information. Generally, the observation of a cross-peak implies that one oscillator responds to the excitation of a different oscillator. This can be due to direct anharmonic coupling, in which case the cross-peak is already visible at $t_1 = 0$. The presence of such a cross-peak between two vibrations shows that the vibrations belong to the same molecule or at least two strongly interacting molecules. Cross-peaks can thus be used to disentangle and assign vibrational spectra of mixtures.[22,31] The polarization dependence of cross-peaks gives the angle between the transition dipole moments of the interacting vibrations, which can be used to determine molecular structure.[32,33] The anharmonic coupling, which can be deduced from the observed anharmonic shifts, can also be used to infer molecular structure.[4,34]

In addition to direct anharmonic coupling, cross-peaks can be created by vibrational energy transfer (VET),[8] in which case they show a time dependence that is different from the time dependence of the diagonal peak of the excited vibration. Usually, VET goes into low frequency modes, which give rise to a cross-peak of the observed high frequency modes through anharmonic coupling.[26] In some cases, direct population transfer between the oscillators linked by a cross-peak has also been discussed.[15,35–37] The time dependence of VET-induced cross-peaks has been used to infer the spatial proximity of oscillators,[26] helping to assign IR spectra,[26,38] and to obtain inter-[39,40] and intramolecular structure information. For VET-induced cross-peaks, the polarization dependence can also be used to obtain transition dipole angles and thus molecular conformation. VET has been shown to frequently create more and stronger cross-peaks then direct anharmonic coupling, thereby considerably increasing the number of useful observables in a 2D spectrum.[26]

The third important mechanism of cross-peak generation is chemical exchange, very much like in NMR exchange spectroscopy (EXSY). If two species exist in dynamic equilibrium and the interconversion of the species leads to a change in the frequency of an oscillator, then a cross-peak is generated between the corresponding absorption bands in the IR spectrum (2D-IR EXSY).[41] The rate of chemical exchange can be deduced from the time dependence of the cross-peak.[12,42] However, the relaxation rate of the excited oscillator has to be in the same range or slower than the rate of chemical exchange, so that the signal does not decay before exchange happens. The investigation of chemical exchange is, therefore, usually limited to an observation window of a few picoseconds. 2D-IR EXSY has been widely used to monitor hydrogen-bond making and breaking[41,43] as well as conformational transitions.[44,45] Chemical exchange usually refers to the situation of discrete, interconverting states. Frequently, a continuous distribution of states, for example, of different hydrogen-bond strengths and angles, exists that leads to inhomogeneous broadening of a band. In the 2D-IR spectrum, such an inhomogeneous distribution leads to a line shape that is elongated along the diagonal of the 2D spectrum. Exchange within this continuous distribution leads to a time-dependent 2D line shape, a phenomenon called spectral diffusion.[46–49] Spectral diffusion can be used to study dynamics in the surroundings of an oscillator, for example, the dynamics of the solvent or a protein environment.[50–54] Energy transfer within an ensemble of oscillators can also cause spectral diffusion.[55–57]

3. Mixed IR/Non-IR Pulse Sequences

As shown in the previous section, a plethora of information is already available from 2D-IR spectroscopy. Adding non-IR pulses expands the possibilities even further and

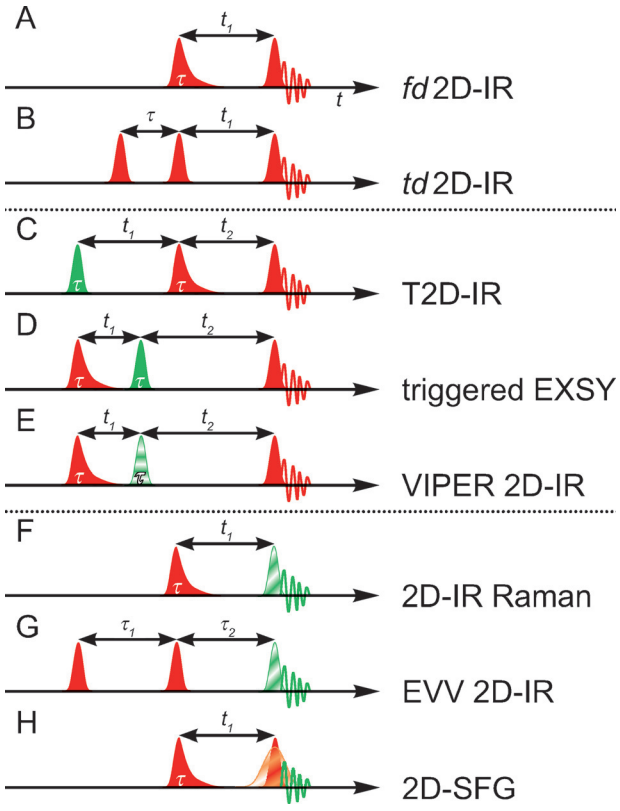

Figure 2. Pulse sequences of the different implementations of 2D-IR and of mixed UV/Vis/NIR-IR spectroscopic methods. The red, green, and orange pulses correspond to infrared, UV/Vis, and NIR light, respectively. The filling of the pulse denotes if it is resonant (filled), nonresonant (diagonally striped), or induced-resonant (horizontally striped). The wavy line represents the to-be-detected emitted field. The thick arrow is the time axis. Intervals labeled with t denote population times, intervals labeled with τ denote coherence times. Pulses with a white τ cause two field interactions and could be replaced by a pulse pair, other pulses cause a single interaction. The 2D-IR acronyms stand for frequency domain (*fd*), time domain (*td*), transient (in T2D-IR), exchange spectroscopy (EXSY), vibrationally promoted electronic resonance (VIPER), electronic-vibration-vibration (EVV, also known as doubly vibrationally enhanced four wave mixing, DOVE), and two-dimensional sum-frequency-generation (2D-SFG), respectively. Some closely related extensions of these experiments are discussed in the respective subsections.

allows for conceptually new 2D vibrational experiments. Figure 2 summarizes most of the currently available mixed IR/non-IR techniques, which feature two vibrational dimensions. They will be discussed in detail in the following subsections. The sequences consist of combinations of resonant IR pulses with resonant (represented by filled pulses) and nonresonant (striped pulses) UV, Vis, or near-IR pulses.

At the top of the figure, the frequency domain (*fd*) and time domain (*td*) implementation of the all-IR 2D experiment are shown. As described above, 2D-IR is a third-order spectroscopy. *fd*2D-IR spectroscopy uses a tunable narrow-band pump pulse for the first two interactions, while *td*2D-IR spectroscopy uses a pair of broad-band pulses separated by the coherence time τ. The tunable narrow-band pulse is usually formed using a computer-controlled etalon, a so-called Fabry–Pérot interferometer. It decays exponentially and is elongated in time compared to the broad-band pulses. To illustrate the equivalence between narrow-band pulses that are responsible for two interactions and the pulse pair, the former pulses are labeled by a white τ in all sequences in Figure 2. Replacing the narrow-band IR pulse by a broad-band IR pulse pair has already been demonstrated for most of the pulse sequences discussed here.

What is the role of the non-IR pulse in the different pulse sequences? Figure 2 shows two general classes of experiments. The first class uses the non-IR pulse for electronic excitation (sequences C, D, and E). Whereas the all-IR 2D experiment (sequences A or B) studies the electronic ground state and is usually applied to a system in equilibrium, these experiments access electronically excited states and allow the study of excited-state dynamics, photochemical reactions with their intermediates and products, photophysical processes, or other phenomena that can be triggered by UV/Vis excitation (e.g. the uncaging of caged compounds, structural rearrangements induced by built-in conformational triggers, dynamics of light-sensitive proteins). In these experiments, a non-equilibrium population is created by the non-IR pulse, which interacts twice with the sample and thus is labeled by a white τ. In total, these experiments are, therefore, fifth-order spectroscopies.

The second class of experiments uses the non-IR pulse for generating different (Raman-type or SFG) probe processes. In the above-mentioned fifth-order experiments, changes in IR absorption are probed (in other words, a polarization that oscillates at IR frequencies is created and measured). In pulse sequences F, G, and H, the signal is measured in the visible spectral range. The UV, Vis, or NIR pulse only interacts once in these experiments to create a suitable polarization. In contrast to the fifth-order experiments, the purpose of the non-IR pulse is thus not to generate a non-equilibrium population. Different selection rules compared to the all-IR 2D experiment or the fifth-order experiments discussed above apply to the Raman-type or SFG experiments and different observables can thus be accessed. Pulse sequences F and G are third-order spectroscopies involving a Raman transition, which allows a broad spectral range (compared to most IR methods) to be probed in one shot, provides access to low-frequency modes, and allows couplings between IR- and Raman-active modes to be measured. Pulse sequence G employs two IR pulses with single interactions with different oscillators (Figure 7) to generate cross-peaks in the case of anharmonic coupling. Pulse sequence H, on the other hand, is a fourth-order spectroscopy, which is surface-specific for symmetry reasons.

The experiments discussed here encompass several interactions with the pulses at different timings to generate third-, fourth-, or fifth-order signals. Lower-order signals generated by molecules which did not experience all the desired interactions need to be suppressed. This can be achieved by mechanical chopping of pulses, selection of beam geometry, phase cycling, and combinations thereof.[4,58,59]

The following subsections discuss in detail the information content of the spectra generated by the pulse sequences in Figure 2, highlighting the effect of the UV, Vis, or NIR pulses in the different cases.

3.1. Transient 2D-IR Spectroscopy

2D-IR spectroscopy (Figure 2 A,B) is typically applied to systems in equilibrium in the electronic ground state. To bring the system into a non-equilibrium state, a UV/Vis pulse can be applied before the 2D-IR spectrum is collected[58] (see Figure 2 C). The information contained in the 2D-IR spectra described in Section 2, such as vibrational couplings and anharmonicities, vibrational lifetimes and energy transfer, spectral diffusion, and exchange, can be obtained for the evolving non-equilibrium system as a function of the waiting time t_1 separating the UV/Vis and 2D-IR pulses.

3.1.1. Structural Dynamics

Applications of the T2D-IR pulse sequence resulted in the characterization of the structure and dynamics of peptides and proteins, such as the isomerization of the chromophore in bacteriorhodopsin,[60] the isomerization of thiopeptides,[61] the structural distributions of a photoswitchable thioreductase active-site fragment,[58,62] and the reorganization of secondary structure in an α-helix and a β-turn.[63,64]

The last study demonstrated that a rigid β-turn in a cyclic disulfide-bridged tetrapeptide opens after UV photocleavage of the disulfide bridge which closes the molecular ring.[63] Evidence for the unfolding mechanism comes from T2D-IR spectra in combination with molecular dynamics simulations. The initially present β-turn contains an intramolecular hydrogen bond. The spectra show a transient cross-peak (labeled TC in Figure 3, particularly evident in the slices in Figure 3 C) appearing after UV irradiation. The cross-peak arises as the hydrogen bond of the β-turn is broken or weakened and the C=O groups of the previously hydrogen-bonded peptide units rotate into a closer position on a 160 ps time scale, in agreement with MD simulations.

In the case of the α-helix, an *S*,*S*-tetrazine constraint has been introduced to perturb the helical structure that is restored upon cleavage of the disulfide bridge.[64] Two neighboring $^{13}C{=}^{18}O$ residues have been introduced at the kink. Their coupling has been extracted from the T2D-IR spectra and used to derive the time-dependent change in the

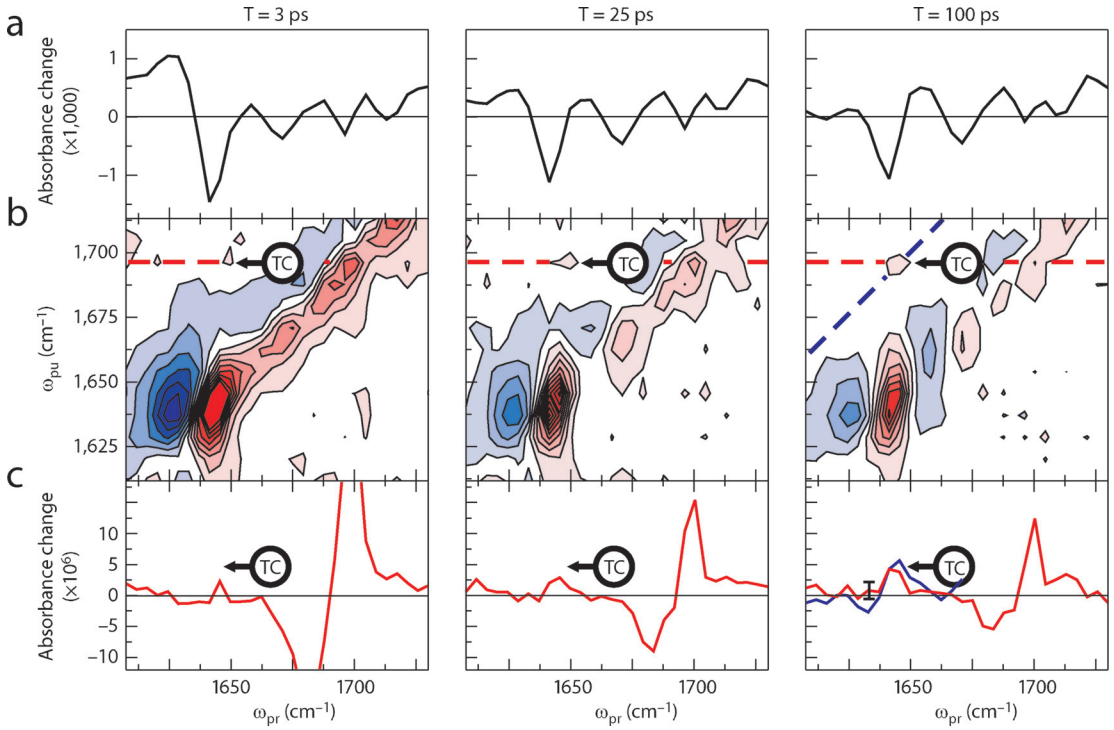

Figure 3. Transient IR and 2D-IR spectra from a small cyclic peptide (cyclo(Boc-CPUC-OMe)) after UV radiation. Transient IR (UV-pump IR-probe) and 2D-IR (UV-IR-IR) spectra at chosen UV delays are shown in panels (a) and (b), respectively. A transient signal (marked with TC) from the carbonyl groups of the initially hydrogen-bonded peptide units that indicates a weakened intramolecular hydrogen bond and leads to the β-turn of the peptide having a looser conformation. The spectra in panel (c) are cuts through T2D-IR spectra along the dashed lines in panel (b). Reproduced from Ref. [63].

dihedral angle of the backbone at the position of the kink. The results reveal motions on the picosecond time scale that restore the helical structure extremely rapidly.

Nanosecond T-jump 2D-IR spectroscopy has already been demonstrated and has been used to investigate protein unfolding[65,66] and nanosecond tautomerization processes.[67] In the T-jump experiment, an overtone of νOH or νOD of the solvent is excited to induce rapid sample heating. As no non-IR pulse is used to directly excite the molecule under investigation, it is beyond the main focus of this Review.

For an example of the structure determination of the photoproduct of the reaction of an inorganic complex see Section 3.1.3.

3.1.2. *Vibrational Dynamics and Solvation of Electronically Excited States*

In addition to revealing structural dynamics, T2D-IR has also proven useful in investigating the coupling between electronic and vibrational degrees of freedom, uncovering energy-redistribution pathways of vibrationally and electronically excited states, as well as investigating the influence of electronic excitation on interactions with the solvent. These possibilities have so far been explored mainly for metal complexes that undergo charge transfer upon electronic excitation.

T2D-IR spectroscopy revealed that VET can differ dramatically between the electronic ground state and the excited state. Weinstein and co-workers found for [Re(Cl)-$(CO)_3$(4,4′-diethylester-2,2′-bipyridine)] that VET between ligands is accelerated by a factor of eight in the electronically excited state.[68] Whereas the VET rates in the ground state are solvent-dependent, the rates in the charge-transfer state are solvent-insensitive. The acceleration of VET in the charge-transfer state is suggested to occur through an efficient intramolecular coupling mechanism that becomes effective. This has been attributed to changed electrostatics and proposed as a general phenomenon for electronic excitation in transition-metal complexes, with implications for their application, for example, in solar energy conversion. A similar acceleration has been observed for [Re-$(CO)_3$(bipyridine)Cl].[69] Changes in vibrational relaxation upon photodissociation have also been investigated.[70] A closely related experiment has been used to study vibrational dynamics upon back-electron transfer in the cyano-bridged transition-metal mixed-valence complex $[(NC)_5Fe^{II}$-C≡N-$Pt^{IV}(NH_3)_4$-N≡C-$Fe^{II}(CN)_5]^{4-}$ after excitation with visible light.[71,72] In this process, higher vibrational states (up to $\nu = 8$) of the investigated modes are populated. Multidimensional spectroscopy revealed the energy flow between modes as the system equilibrates after electron transfer.

Electronic excitation may lead to considerable charge redistribution; therefore, interactions with the solvent frequently play an important role. Solvation processes can be probed in great detail by monitoring the time-dependence of 2D line shapes, which reflects the dynamics of the solvent

around the probed vibration ("spectral diffusion"). Kubarych and co-workers applied this to a photocatalyst in its electronic ground and excited state.[69] A threefold decrease in spectral diffusion upon electronic excitation is observed, which is attributed to the changed electrostatics. A widely used method for investigating solvent dynamics is based on the observation of the dynamic fluorescence Stokes shift. Whereas Stokes shift measurements mix ground state and excited-state dynamics by probing the energy gap, T2D-IR spectroscopy can address each state separately.[69] Furthermore, local information can be obtained for oscillators located at different sites of the molecule. A wider range of processes can be investigated, including for example, photoreactions where fluorescence does not occur.

3.1.3. Disentangling Photochemical Reaction Mixtures

Possibly the most obvious application of T2D-IR is the investigation of a photoreaction induced by a UV/Vis pulse. Chemically distinct transient species can consequently be identified, such as different isomers.

The photoreaction induced by UV irradiation has been investigated for a [FeFe]hydrogenase enzyme model compound [(μ-propanedithiolate)$Fe_2(CO)_6$].[73] The observation of cross-peaks between product bands has been used to prove that all of the product bands belong to the same species. This is a clear proof that only a single photoproduct is generated. Moreover, the polarization dependence of the T2D-IR signal has been used to infer the transition dipole angles of vibrational modes in the product. Comparison between experimentally determined and computed angles revealed that an axial CO group has been substituted by solvent. Structure determination of intermediates and products, as demonstrated here, has great potential to become an important application of T2D-IR spectroscopy.

T2D-IR has been used to study geminate rebinding of a metal-carbonyl dimer, and revealed that only one of the two specific isomers of the geminate complex can be the precursor of the reformed ground state.[74] This particular experiment induces the formation of radical monomers after photoexcitation ($\lambda_{ex} = 400$ nm) of a molybdenum cyclopentadienyl carbonyl dimer [{$CpMo(CO)_3$}$_2$], produced by cleavage of the Mo–Mo bond. The dimer can exist in *trans* and *gauche* conformations. The central frequency of the C=O vibration is conformer-specific (the linear absorption spectrum shows bands at 1912 cm^{-1}, 1958 cm^{-1}, and 2013 cm^{-1}). The highest wavenumber band corresponds to the *gauche* conformation only. Nevertheless, the 2D-IR spectra show cross-peaks between all three bands, thereby revealing that the lower wavenumber bands have contributions from both the *gauche* and *trans* conformers. Both conformers can be photocleaved. The T2D-IR spectrum recorded after 5 ps (not shown here) shows that radicals are formed. The observation of partial bleach recovery at 1958 cm^{-1} and no recovery at 2013 cm^{-1} demonstrates that the *gauche* form is not responsible for radical recombination and only the *trans* form is generated. In combination with quantum chemical computations, it is concluded that this isomer channel is already preselected at very large Mo bond distances.

A very powerful approach for disentangling reaction pathways of coexisting species is the triggered exchange experiment discussed in Section 3.2.

3.1.4. Steering Reactions

The vibrations excited during a T2D-IR experiment can not always be treated as spectators. When they are part of the reaction coordinate, their excitation can influence the outcome of the reaction initiated by the UV/Vis excitation. This has been elegantly demonstrated by Weinstein, Towrie, and co-workers using the T2D-IR pulse sequence.[75] In their experiment, they modulated electron transfer (ET) in a donor-bridge-acceptor (DBA) system by exciting a distinct vibration of the bridge with a tunable narrow-band IR pulse after UV excitation (Figure 4). Excitation at 400 nm creates

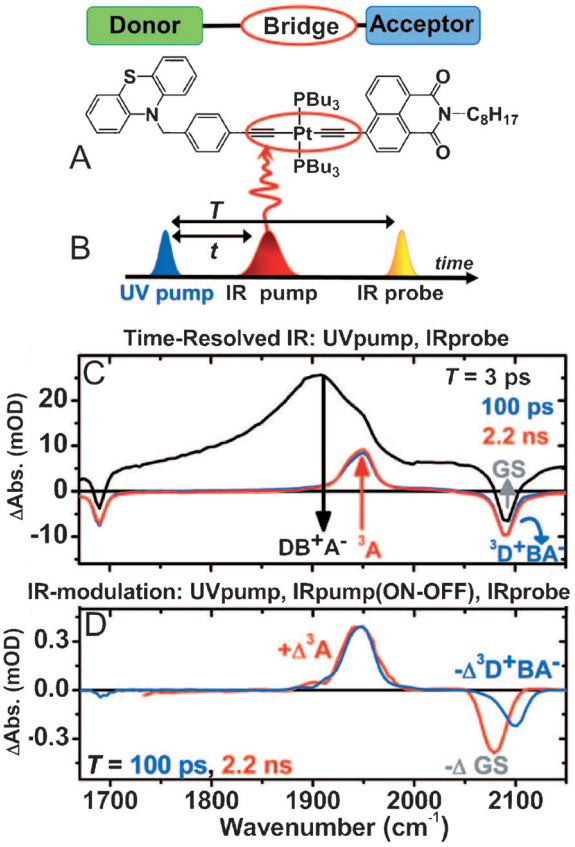

Figure 4. Control of ET pathways by IR excitation at 1908 cm^{-1} using the T2D-IR sequence. The top panel shows the time-resolved IR spectra at representative delay times. The bottom panel shows the difference spectra Abs(IR_{pump}ON) − Abs(IR_{pump}OFF) at $T = 100$ ps and 2.2 ns after UV_{pump} excitation (UV_{pump} − IR_{pump} delay t fixed at 2 ps) that demonstrate suppression of the $^3D^+BA^-$ pathway and an increase in the ^3A pathway by IR excitation. Reprinted from Ref. [75] with permission from the AAAS.

a charge-transfer state (DB^+A^-), which can decay into a π-π* intraligand triplet state (^3A) on the naphthalene imide ligand, a charge-separated state ($^3D^+BA^-$), or into the ground state (GS). By excitation of the bridge C≡C vibration, formation of

the ^{3}A state is enhanced at the expense of formation of the charge-separated $^3D^+BA^-$ state. This is nicely illustrated by the double difference spectrum of the signal with and without IR_{pump} excitation (Figure 4D, blue spectrum), which shows an increase of the ^{3}A signal and a decrease of the $^3D^+BA^-$ signal upon IR excitation. At longer times (Figure 4D, red spectrum), IR excitation leads to an increase of ^{3}A at the expense of GS recovery. If the IR excitation is tuned to the ν(C=O) vibration localized on the acceptor in the same DB^+A^- excited state (or to an IR absorption band of the solvent), it does not exhibit any effect. Scanning the wavenumber of the IR_{pump} pulse across the transient IR band of the C≡C vibration in the DB^+A^- excited state (Figure 4C, band centered at 1900 cm^{-1}) reveals that the magnitude of the effect follows the band shape of the excited state. Quantitative analysis revealed that the $^3D^+BA^-$ channel can be completely switched off by vibrational excitation. In a different system, acceleration of charge transfer upon vibrational excitation of a single mode of the donating ligand has been reported.[76]

3.1.5. Outlook

For the investigation of non-equilibrium dynamics by 2D-IR spectroscopy, other triggers besides electronic excitation can be envisioned, such as fast pressure jumps (to induce protein dynamics, for example,[77,78] pH jumps (a pH change can be induced using photo acids),[79,80] stopped-flow methods (to study protein folding with millisecond time resolution),[81] change of redox potential, or external electric or magnetic fields. The application of synchronized femtosecond lasers for generating the various pulses will allow a broad range of time scales to be covered.[82]

T2D-IR spectroscopy bears great promise for the investigation of photochemical reaction mechanisms, as it has the potential to provide very detailed information on the structure and dynamics of intermediates and products. As illustrated by the examples in this section, the extraction of structural information from T2D-IR spectra has so far mostly remained on a relatively coarse level. For systems in equilibrium, very detailed determination of structures by 2D-IR spectroscopy has already been demonstrated.[31–34,83] T2D-IR spectroscopy opens the possibility to also reach this level of detail for transient species, where the high time resolution of femtosecond spectroscopy can be put to full use.

The idea of directly exciting vibrations to steer a photochemical reaction opens up new possibilities for investigation of the interaction between nuclear and electronic degrees of freedom. Although current studies employed narrow-band IR pulses, the use of mid-IR pulse shaping[84] to design wave packets for more elaborate control would be an exciting extension.

3.2. Non-Equilibrium or Triggered 2D-IR Exchange Spectroscopy

An intriguing pulse sequence is the triggered 2D-IR EXSY sequence of Figure 2D,[85] where the UV/Vis and IR pulses are reversed so that the IR pulse arrives at the sample first. The influence of the IR pulse on the vibrational spectrum of the electronic ground and excited state can thus be followed. The pulse sequence correlates vibrations of the reactant and the product (or intermediate) by "labeling" a specific vibrational mode with narrow-band infrared excitation, after which a resonant UV/Vis pulse at t_1 is applied for electronic excitation, followed by the IR probe pulse to measure the spectrum.[85,86] In this fashion, cross-peaks are generated between related vibrations of the reactant and product. This approach has also been termed triggered exchange spectroscopy.[87] Replacing the narrow band IR pump pulse by a pulse pair has been demonstrated as well.[87] In the classical 2D-IR EXSY experiment, which uses the pulse sequences in Figure 2A,B, thermal motion drives the system from one state to the other during the population time t_1 between IR pump and IR probe interactions. In the triggered exchange experiment, the UV/Vis pulse applied during the waiting time drives the system from one state to the other. Related experiments, which create cross-peaks between reactant and product spin transitions have been demonstrated in NMR spectroscopy.[88,89] Instructive applications of triggered 2D-IR EXSY discussed here are the investigation of charge injection by an inhomogeneous ensemble of dye molecules on a nanocrystalline film[90] as well as light-induced ligand migration in coexisting protein conformers.[86]

In the first example, optical excitation of a Re dye occurs through a Vis pulse ($\lambda_{ex} = 400$ nm) that induces charge transfer to a nanocrystalline TiO_2 film (Figure 5a). The dye's excitation and charge injection processes are then followed by T2D-IR spectroscopy. Probing of the electronic ground state by 2D-IR spectroscopy reveals three diagonal peaks in the a′(1) symmetric CO stretch region in Figure 5a (at 2020 cm^{-1}, 2030 cm^{-1}, and 2042 cm^{-1}). The fact that no cross-peaks exist shows that the peaks originate from three different structural arrangements of the dye on the surface. Furthermore, the absence of cross-peaks shows that this heterogeneity is not a consequence of dye aggregation, in which case the close-lying molecules would be coupled and cross-peaks would be generated. Electron transfer is initiated by Vis excitation (the Type-I sequence in Figure 5b, corresponding to T2D-IR in Figure 2C, but using a pulse pair for IR excitation instead of a narrow-band pulse). All three ground-state diagonal peaks respond to excitation, but only one excited-state feature at 2060 cm^{-1} emerges (see Figure 5c, ①). After changing the relative delays to pulse sequence Type-II (Figure 5b, corresponding to triggered 2D-IR EXSY in Figure 2D), a broad cross-peak appears (Figure 5d, ②) that links the two ground-state bands at 2020 cm^{-1} and 2030 cm^{-1} to the excited-state band at 2060 cm^{-1} (arrows). The corresponding cross-peak for the 2042 cm^{-1} band is missing (arrow and cross). In this way, the triggered 2D-IR EXSY experiment reveals that the observed electronically excited state is generated only by two out of the three dye conformations. As long-lived ground-state bleaches are generated for all three conformations, the authors conclude that the dye conformations at 2020 cm^{-1} and 2030 cm^{-1} undergo slow charge injection and the electronically excited state can be observed in the 2D-IR (and transient IR) spectrum, while the conformation at 2042 cm^{-1} undergoes

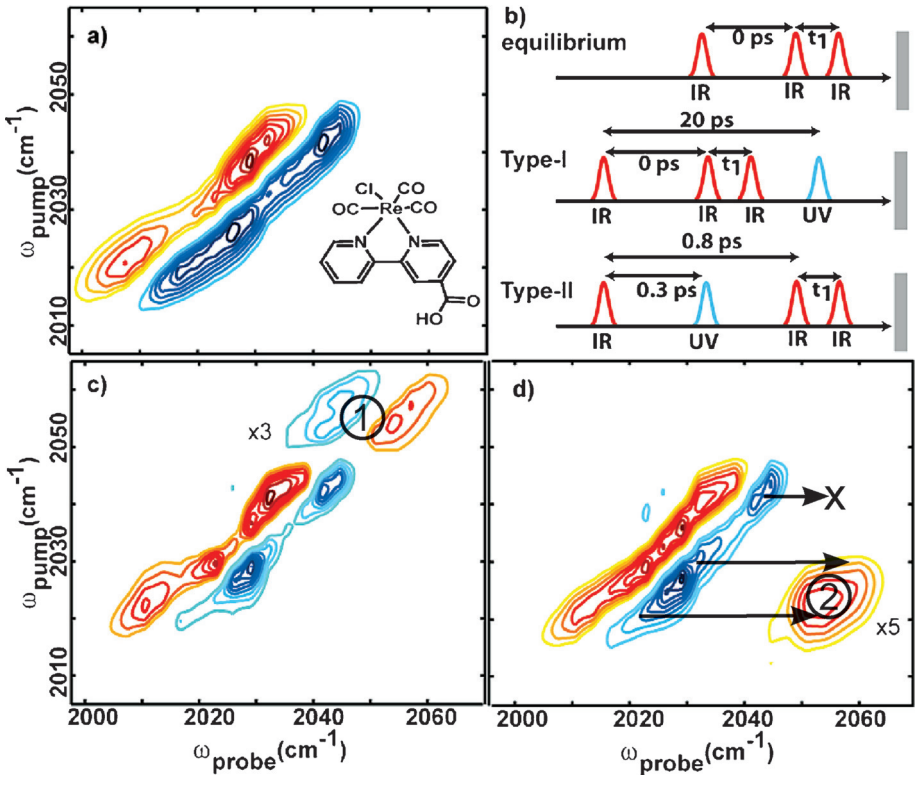

Figure 5. Charge injection in a TiO_2 film sensitized with a Re dye. A) Equilibrium 2D-IR spectrum of the system. B) Pulse schemes used to obtain spectra (a), (c), and (d). Pulses are shown as they propagate towards the sample, in contrast to Figure 2, where the pulses are plotted on the time axis. Furthermore, a pulse pair is used for excitation, while in Figure 2 the experiments are displayed with a narrow-band IR pump instead. Adapted from Ref. [90]. Copyright 2009 American Chemical Society.

very fast injection, thus the excitation localized on the dye is not observed.

The second example investigates the migration of a carbon monoxide ligand through protein (myoglobin) pockets after photorelease from its binding site.[86] Information is obtained about the local surroundings of the ligand by monitoring the stretching frequency of the ligand, thereby uncovering the existence of various CO bands. The different bands of CO at the binding site (called A_3- and A_1-states in the literature) have been attributed to different protein conformations. Upon photorelease, the so-called B-states, which correspond to CO in the protein pockets, are populated. By using triggered 2D-IR EXSY, it has been possible to correlate docking-site bands and binding-site bands through the cross-peaks, thereby revealing which of the observed docking site signals belongs to which protein conformation. Before the development of triggered 2D-IR EXSY, it was attempted to obtain such information by spectroscopy on protein mutants that shift the equilibrium between conformations, which led, however, to ambiguous results. Triggered 2D-IR EXSY provided a spectroscopic solution to that problem and has permitted the identification of connectivities between substates (bound CO substates connected to unbound CO substates) where multiple conformations are possible.

Outlook

The above examples illustrate that the photochemistry or photophysics of different coexisting species, such as protein conformers or molecules populating different sites on a surface, can be selectively investigated by triggered 2D-IR EXSY. This application of the triggered exchange approach also has been adopted in 2D-Vis spectroscopy.[91] Another option with high application potential offered by triggered 2D-IR EXSY is the assignment of vibrational bands of electronically excited states, intermediates, or products, starting from a known reactant spectrum by generating cross-peaks between vibrations of the reactant and the transient species.[85] This is an extremely valuable feature for disentangling the spectra of photochemical reaction mixtures.

An important limitation of triggered 2D-IR EXSY is that the cross-peak can only be observed within the life time of the vibrationally excited state that is generated by the IR pump pulse. This is a severe constraint, because it limits the applicability of triggered 2D-IR EXSY to processes that are on the same time scale or faster than the vibrational life time. Typical life times are below 5 ps, in exceptional cases they can be much longer (e.g. tens of ps for CO in metal carbonyls or hundreds of ps for CO migrating inside a protein). The limitation posed by vibrational lifetime can be overcome using the VIPER-2D-IR pulse sequence discussed in Section 3.3.

3.3. VIPER 2D-IR Spectroscopy

The VIPER 2D-IR sequence (see Figure 2E)[59] consists of an infrared excitation that is resonant with a vibrational mode, followed by an off-resonant UV/Vis pulse at t_1. The UV/Vis pulse is tuned to be only resonant with the vibrationally excited species. Thus, reaching the electronic excited state requires both IR and subsequent UV/Vis excitation of the molecule. Only the subset of molecules in a mixture that is selected by the narrow band IR pulse is electronically excited. Figure 6B illustrates this double resonant excitation. VIPER 2D-IR spectroscopy is, therefore, substantially different from triggered 2D-IR EXSY (Figure 2D) which uses a resonant UV/Vis pulse. The evolving system is then probed in the infrared region after t_2. The 2D-IR signal generated in this fashion decays, therefore, with the electronic life time, which in many cases is substantially longer then the vibrational life

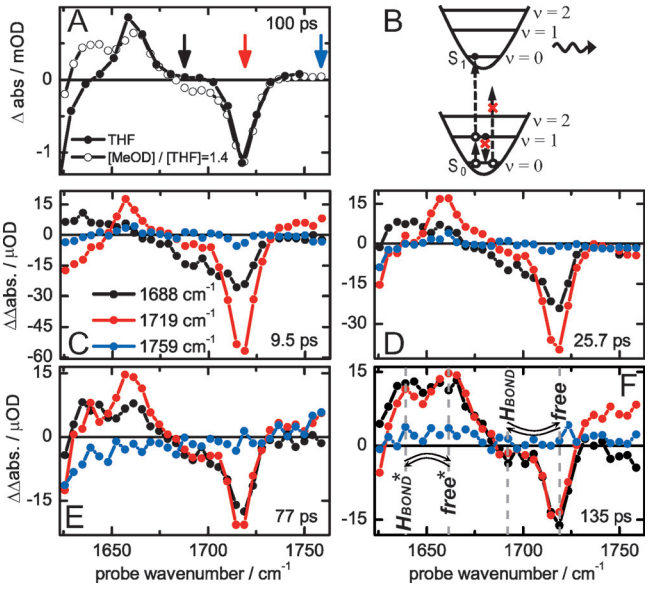

Figure 6. Chemical exchange of species beyond the vibrational lifetime. A) Transient IR spectra of coumarin 6 in THF in the carbonyl region, with and without deuterated methanol. B) Energy level diagram that illustrates the VIPER double-resonant excitation. The off-resonant Vis pulse (dashed line) comes shortly after the resonant IR pulse to reach S_1. Vibrational relaxation back to the ground state is suppressed (crossed-out downward arrow). The Vis pulse alone (crossed-out upward arrow) is not sufficient to reach the excited state. C–F) Slices of transient VIPER 2D-IR spectra of a mixture (with MetOD) that are collected at different IR pump frequencies (colored arrows in (A)). Reproduced from Ref. [59]. Copyright 2014 Wiley-VCH Verlag GmbH & Co. KGaA, Weinheim.

time. In the case where a permanent change of the molecule is caused by the UV/VIS pulse, for example, by photochemistry (wavy arrow in Figure 6B), the life time of the signal is even "infinite". A requirement for application of the VIPER 2D-IR pulse sequence is that the UV/Vis spectrum of the molecule is modulated by IR excitation. As a consequence, in VIPER 2D-IR spectroscopy, the information that a molecule has been vibrationally excited is stored in the electronic degree of freedom. Some molecules in the sample might be directly excited by the UV/Vis pulse without IR excitation; however, this background can be subtracted using an appropriate chopping scheme.[59]

3.3.1. *Exchange Beyond the Vibrational T_1 Time*

The regular 2D-IR EXSY experiment reveals exchange between different molecular species driven by thermal motion, such as, for example, the interconversion between conformers.[42] The triggered exchange experiment discussed in Section 3.2 can correlate vibrations before and after an interconversion that is triggered by electronic excitation. Both methods rely on labeling a vibration by exciting it and tracking the wavenumber of the excited vibration to observe the interconversion process. Therefore, the observation window is limited by the vibrational life time. This essential limitation can be circumvented by VIPER 2D-IR spectroscopy. As described above, the VIPER signal decays not with the vibrational but with the electronic lifetime (or even not at all, in the case where the system is permanently modified by the UV/Vis pulse).[59]

VIPER 2D-IR spectroscopy has been demonstrated by resolving chemical exchange between hydrogen-bonded and free molecules of coumarin 6 in a mixture, where exchange takes substantially longer then the vibrational life time.[59] Transient IR spectra of the carbonyl vibration of the coumarin 6 laser dye have shown that the addition of methanol results in the appearance of a second species that absorbs at lower frequencies, both in the electronic ground and excited states (evident by the negative and positive peaks in Figure 6A, respectively).[59] In the new species, the carbonyl group is hydrogen bonded to the alcohol (see Figure 6F for the labeling of the bands). By using a narrow infrared pump pulse, one can select which species (hydrogen bonded or free) to promote to the electronic excited state.

Figure 6C–F shows cuts through the VIPER 2D-IR spectra as a function of time. The red (black) spectrum corresponds to the IR pump pulse being tuned to the free (hydrogen-bonded) species. Exchange between free and hydrogen-bonded species occurs both in the electronic ground state and in the excited state, as indicated by the arrows in Figure 6F. The exchange is complete when the black and red spectra have the same shape (as in Figure 6F). This is the case after about 135 ps. Note, that the vibrational life time of the carbonyl vibration is only 1.2 ps, which is why regular 2D-IR EXSY cannot be used for this system.

3.3.2. *Outlook*

Comparison of the red VIPER 2D-IR spectrum in Figure 6C, collected from a mixture of hydrogen-bonded and free molecules, to the black time-resolved IR spectrum in Figure 6A, collected from a solution with only free molecules, shows that it is possible to select a species (in this case not hydrogen-bonded molecules) out of a mixture, selectively photoexcite it, and record its transient absorption spectrum. In the Vis spectrum, the absorptions of different populations of molecules (e.g. hydrogen bonded versus free) often strongly overlap and selective Vis excitation is difficult or even impossible. The VIPER sequence overcomes this problem by selective IR pre-excitation of one of the species in the mixture. The chosen (i.e. vibrationally excited) population interacts with the off-resonant visible pulse that brings the vibrationally excited molecules to the excited state. In this fashion it is possible not only to investigate exchange, but also to investigate the photochemistry or photophysics of coexisting molecules, even if their UV/Vis spectra are very similar, which is frequently the case, for example, for conformers or molecules in slightly different environments and even if the coexisting molecules are in fast dynamic equilibrium. Triggered exchange spectroscopy can provide similar information, however, only over the very short time window of the vibrational life time. The VIPER experiment, in contrast, will allow the whole light-triggered process for selected sub-ensembles to be tracked. This might not only be interesting for time-resolved spectroscopy but also for carrying out selective photoreactions.

3.4. Multidimensional IR-Raman Spectroscopies

All the pulse sequences discussed above probe IR transitions. If instead a Raman transition is probed after IR excitation (see Figure 2F,G), correlations between IR and Raman bands can be investigated. This is achieved by recording the Raman scattering of a visible probe pulse, after one or more resonant infrared pulses have interacted with vibrational modes.

3.4.1. 3D IR-Raman Spectroscopy of Vibrational Dynamics

The technique known as 3D-IR-Raman spectroscopy[92–94] (see Figure 2F) is in the context of this Review a 2D technique, as the spectra depend on *two* vibrational frequency variables and the third dimension is time. The 3D-IR-Raman experiment is a third-order spectroscopy that uses an IR pump pulse for excitation and incoherent Stokes and/or anti-Stokes Raman scattering of a Vis pulse for probing. In the beginning, the lack of means to detect vibrational excitations directly in the IR range was a driving force for the development of this experiment. The main application of this experiment so far has been the investigation of vibrational energy redistribution (VER). Typically, a high-frequency mode is excited and the subsequent vibrational dynamics is investigated by measuring the time dependence of cross-peaks with other vibrations. While this is also possible using conventional 2D-IR spectroscopy,[26,38] the 3D-IR-Raman approach has certain strengths. Most importantly, a broad spectral range can be probed simultaneously by Raman detection and many of the low-frequency modes receiving vibrational energy can be directly observed. Furthermore, the incoherent Raman signal comes only from vibrationally excited states without contributions from ground-state holes which complicate the regular 2D-IR spectra.[93] A downside of 3D-IR-Raman is its very low sensitivity. Very high concentrations or bulk liquids are typically used. The necessity of intense pulses often requires the use of liquid jets, and various artifacts have to be taken into account.[95] The transitions probed by this Raman detection scheme are complementary to IR detection methods, because the transitions are based on different selection rules. Detailed investigations of VER along alkyl chains,[96] across micelles,[97] of water vibrational dynamics,[98] of DNA base pairs,[99] as well as of the effect of chemical modifications on vibrational dynamics[100,101] have been carried out using this experiment.

3.4.2. DOVE or EVV 2D-IR Spectroscopy

The IR-IR-Raman sequence (see Figure 2G), called DOVE FWM (doubly vibrationally enhanced four-wave mixing) or EVV (electron-vibration-vibration) 2D-IR spectroscopy,[27,102–104] is also a third-order spectroscopy and contains two IR pulses and a Vis pulse. In the EVV process, two infrared transitions and a Raman transition occur as a result of the presence of IR pulses with frequencies ω_α and ω_β and a Vis pulse with ω_γ (Figure 7). The signal is detected at ω_δ. Accordingly, IR and Raman selection rules apply for the different interactions.[27] It is a coherent experiment that does not involve population periods. Cross-peaks are generated when the IR pulses are independently in resonance with two anharmonically coupled vibrations. The vibrations may be located on the same or on different molecules. Coupling can arise from mechanical and/or electrical anharmonicity. As EVV 2D-IR spectroscopy is not a difference spectroscopy, the visibility of the cross-peaks does not depend on the size of the anharmonic shift, which is the case for conventional 2D-IR spectroscopy, where excited-state and ground-state contributions cancel in cases where the anharmonicity is too small. By using different pulse orderings for the two IR pulses, thereby switching between diagram 1 or diagram 2 and 3 in Figure 7, vibrational cross-peaks could be measured either at the frequencies of the base vibrational states or split by the coupling energy,[105] which can help to simplify spectra.

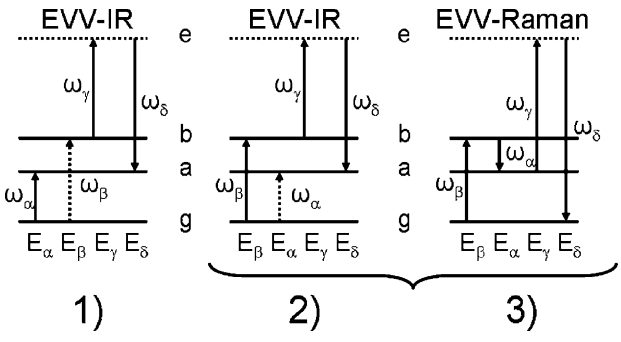

Figure 7. Energy-level diagrams for EVV 2D-IR spectroscopy. E_α and E_β are the IR fields, E_γ is the Vis field, and E_δ is the detected four-wave-mixing (FWM) field. When the IR fields are resonant, the FWM signal is enhanced. Reprinted from Ref. [102]. Copyright 2009 American Chemical Society.

Detection of Intermolecular Contacts and Geometry

A particular advantage of the EVV 2D-IR approach for investigating weak intermolecular interactions compared to 2D-IR spectroscopy is its sensitivity to through-space, electrically mediated vibrational coupling. Coupling cross-peaks between vibrations localized on different molecules can be observed and used for geometry determination. This has been demonstrated for the formation of a complex between phenylacetylene (PA) and benzonitrile (BN).[106,107] A direct comparison of the spectra from both components individually and a mixture of those two reveal cross-peaks that are not present for the single components (see Figure 8). Not only the relative orientation but also the distance between molecules can be determined by EVV 2D-IR spectroscopy, which reveals a distance of 3.60 Å between the CC and CN bond centers and an angle of 31° between bond vectors.[107]

Optical Fingerprinting of Peptides and Proteins

2D spectroscopy enhances specificity compared to 1D spectroscopy by spreading wavenumber-dependent information over two dimensions. The capability of EVV 2D-IR to

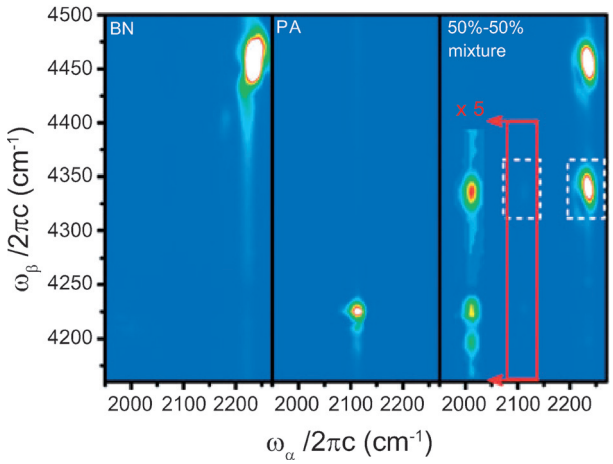

Figure 8. Experimental EVV 2D-IR spectra of pure liquid benzonitrile (BN), phenylacetylene (PA), and a 50:50 mixture of those two compounds. The red box is multiplied by a factor of five and shifted for clarity. The cross-peak at 2225/4465 cm^{-1} is between the CN stretching fundamental of BN and its first overtone (left panel), the cross-peak at 2110/4226 cm^{-1} is between the CC stretching fundamental of PA and its first overtone (middle panel). The mixture shows two new cross-peaks at 2110/4335 and 2225/4335 cm^{-1} (CC-CN and CN-CC cross-peaks), caused by electrical anharmonicity induced by through-space interaction between the CC and CN groups.[106] Reproduced in part from Ref. [106] with permission from The Royal Society of Chemistry.

further decongest spectra compared to 2D-IR is also advantageous for optical fingerprinting of peptides and proteins. In fingerprinting, a library of reference spectra (i.e. the fingerprints) of individual amino acids is built to permit the unambiguous determination of their presence and concentration in a mixture of unknown composition. To this end, a study has used a library of characteristic signals for CH_2 and CH_3 bands, and has determined the relative quantities of phenylalanine, tyrosine, and tryptophan in proteins. In addition to protein identification, absolute quantification of protein levels has also been shown to be possible.[108,109] Application for the investigation of posttranslational modifications based on characteristic cross-peak patterns has also been suggested[102] and demonstrated for the quantification of tyrosine nitration in peptides.[110]

Imaging with Chemical Contrast

Imaging with chemical contrast is of considerable interest in a variety of fields. Chemical contrast means that the contrast in the image is determined by the presence or absence of a certain molecule or functional group. Regions where the concentration of the molecule or group (e.g. within a cell) is high appear bright and where it is low appear dark. Established approaches are based on one-dimensional spectroscopy, such as IR, Raman, and CARS. These approaches, however, suffer from spectral congestion. The extra dimension of EVV 2D-IR spectroscopy considerably decongests spectra. Furthermore, high spatial resolution can be obtained compared to IR microscopy as the location of signal generation depends on the Vis pulse, which can produce a tighter focus. A proof-of-principle experiment has shown the possibility of visualizing the distribution of hematoxylin in kidney tissues by recording a specific cross-peak signal,[102] as well as the distribution of proteins.

3.4.3. Outlook

In the above applications, the Raman pulse is nonresonant with an electronic transition. Enormous signal amplification can be obtained if resonance-Raman detection is exploited.[102] The resonance-Raman effect is used, for example, in the TRSF (triply resonant sum frequency spectroscopy) method, a fully coherent third-order spectroscopy using two resonant IR pulses and one resonant UV/Vis pulse. TRSF has been shown to be effective in measuring 2D spectra at low concentrations (50 μM) of the styryl 9M laser dye in a solvent (i.e. deuterated acetonitrile), even though the steady-state IR absorption spectrum of the sample does not shown any dye features, as the IR absorption bands are below 0.1 mOD.[111] Vibrational states provide excellent spectral selectivity, whereas electronic states provide large resonance enhancements and high spatial resolution in microscopy. The increase in sensitivity requires a suitable electronic transition, but can be of great importance for biological applications, such as the fingerprinting application described here, in which the concentration of proteins, metabolites, or drug molecules to be detected is low and potentially many different substances are present.

3.5. Interface-Specific 2D-SFG Spectroscopy

Many chemical, biological, and physical processes, such as heterogeneous catalysis, transport through cell membranes, and charge injection in solar cells, occur at interfaces. 2D-SFG spectroscopy targets exactly those interfacial systems that are difficult or impossible to probe by bulk methods such as 2D-IR spectroscopy, and is able to deliver sub-monolayer sensitivity (Figure 9).[112] 2D-IR spectroscopy is a nonspecific method in that it generates signals both from the interface and bulk, where typically the bulk signal overwhelms the signal from the surface. By making use of sum-frequency generation of IR with NIR light (see Figure 2H) it is possible to generate

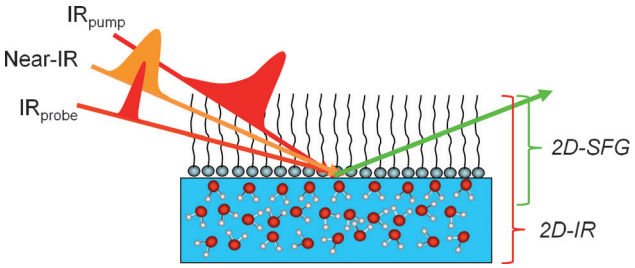

Figure 9. 2D-SFG experiment. The two IR pulses impinge on the surface. A 2D-IR signal is generated from the bulk and surface. Up-conversion by the near-IR pulse to the Vis spectral range only occurs for vibrations which do not have a mirror image counterpart, hence the bulk typically does not contribute.

signals in an interface-specific fashion, because a non-centrosymmetric system is required for the nonlinear process.[113,114] After an initial vibrational excitation, a third-order vibrational coherence is created which could be measured in the infrared spectral region after t_1. A simultaneously arriving nonresonant near-IR pulse at t_1 up-converts the coherence through sum-frequency generation to the Vis spectral range, thus making it a fourth-order coherence.[112,115] The first implementation of 2D-SFG spectroscopy used homodyne detection of the emitted Vis signal.[112] In homodyne SFG detection, the quadratic dependence of the signal on the number of oscillators and interference of the signals emitted by different oscillators can lead to very complicated spectra, even with cross-peaks between uncoupled vibrations.[117] Heterodyne detection removes these complications and is required to obtain 2D-SFG spectra which are equivalent to 2D-IR spectra, thus allowing for phase-sensitive measurements and line shape analysis as well as measuring anharmonic shifts.[117–120] The advantages of 2D-SFG spectroscopy are that it gives background-free signals and highly efficient Vis CCD detectors can be used, similar to what has been done to collect 2D-IR spectra through chirped-pulse upconversion.[116] Conventional 2D-IR experiments on surfaces have been demonstrated for situations where bulk signals are small or absent and the probed vibrations have high transition dipole moments (e.g. on metal carbonyls or other small molecules in proximity to gold surfaces or silica layers).[121–125] With 2D-SFG spectroscopy, the whole range of information available from bulk 2D-IR experiments can now be obtained for a large variety of surfaces and interfaces.

3.5.1. *Structure and Dynamics of Water at Interfaces*

As a consequence of the large number of reactions occurring at the water interface, for example, in atmospheric chemistry or the proximity of membranes, the structure and dynamics of the water interface is of great interest. The 2D-SFG method has recently given insight into the different water structures and dynamics at the water-air and water-lipid interfaces.[119,120,126] Spectral diffusion in 2D-SFG measurements of the water-air interface revealed the existence of an inhomogeneous ensemble with weaker and stronger hydrogen-bonded molecules.[126] A particular hydrogen-bonded water species with an OH stretch wavenumber of 3500 cm^{-1} or above was identified which shows comparably slow spectral diffusion (540 fs), much slower than that of bulk water (50–180 fs) or other surface species in the wavenumber range from 3200 to 3400 cm^{-1} (240 fs). The authors concluded that these hydrogen-bonded OH oscillators belong to water molecules where the other hydrogen atom points towards the air and is not involved in a hydrogen bond. Their modes are more localized and spectral diffusion is not dominated by Förster-type energy transfer, as in bulk water, but is governed by structural dynamics. The rearrangement of hydrogen bonds with these water molecules seems to be relatively slow. Further support for this assignment of the 3500 cm^{-1} portion of the spectrum comes from a study where the free OD oscillators pointing into the air were excited (heavy water was used, thus wavenumbers are not directly comparable).[119] They show an instantaneous cross-peak with the blue side of the spectrum of hydrogen-bonded hydroxy groups, corresponding to the 3500 cm^{-1} species, which can be attributed to intramolecular coupling.

The 2D-SFG response of the water-lipid interface (see Figure 10) has been measured to be different from that of the water-air boundary.[127] In this study, heavy water has been used to shift the hydroxy stretch frequency to about

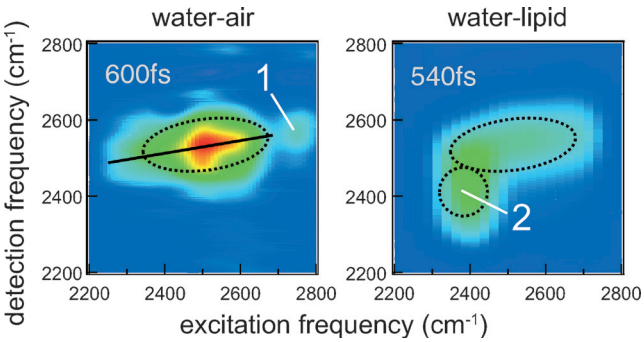

Figure 10. 2D-SFG spectra of the water-air interface and water-lipid (1,2-dipalmitoyl-3-trimethylammonium-propane; DPTAP) interface in the νOD region show different spectral features that reveal different structures at the interface. Interestingly, the 1D-SFG spectra of the two interfaces (not shown) look much more similar.[124] Note that the pump and probe wavenumber axes are swapped compared to the other figures in this Review. Reprinted from Ref. [127]. Copyright 2011, AIP Publishing LLC.

2500 cm^{-1}. Although the 1D-SFG spectra of the water-air and water-lipid interfaces look quite similar (not shown), the 2D-SFG spectra are remarkably different. In accord with the bulk absorption spectrum, the 2D-SFG spectrum of both the water-air and the water-lipid interface shows a broad band at 2500 cm^{-1}, which corresponds to hydrogen-bonded water molecules (the ellipse in Figure 10). Interestingly, the water-air spectrum reveals the presence of free hydroxy groups at an excitation wavenumber of 2750 cm^{-1} (peak 1 in Figure 10, the labeled peak is the cross-peak between free and hydrogen-bonded hydroxy groups, the diagonal peak above is faint).[119] This signal is absent from the spectra of the water-lipid system, but the spectra exhibit a peak of strongly hydrogen-bonded water molecules at 2400 cm^{-1} (peak 2 in Figure 10). This signal has been attributed to water molecules that are strongly hydrogen bonded to the lipid head groups. Time-dependent spectra show that these lipid-bound molecules are largely decoupled from the water layer next to the membrane (ellipse in the water-lipid spectrum of Figure 10). No energy transfer or exchange of water molecules on a picosecond time scale is observed.

3.5.2. *Outlook*

The application of 2D-SFG spectroscopy to systems other than water is still in its infancy. The studies carried out on water have so far put their focus on spectral diffusion and energy transfer. As illustrated by theoretical studies, the 2D-SFG method, however, has the potential to yield information

on the structure, orientation, and dynamics of molecules at interfaces by measuring their anharmonic couplings, vibrational lifetimes, 2D line shapes, and polarization dependence of the signals, in analogy to the achievements of regular 2D-IR spectroscopy for bulk systems.[128–131] By analyzing the phase, even the absolute orientation of transition dipoles is available.[132,133]

The first studies beyond water targeted peptides on surfaces.[134,135] For a peptide that was found to be largely α-helical in solution, 2D-SFG revealed that the peptide largely remained α-helical even on a gold surface (concluded from the small anharmonicity of the amide I band and the homogeneous line shape, which rules out denaturation) and assumed an upright orientation.[134] Another example tracked the formation of amyloid fibers on a functionalized gold surface.[135] Many important areas of application can be foreseen for 2D-SFG spectroscopy, such as energy flow at interfaces,[136] interfacial systems in the context of solar energy conversion, heterogeneous catalysis, reactive surface layers and adsorbates, electrochemistry, and molecular electronics.

4. Summary and Outlook

The range of applications of 2D-IR spectroscopy enhanced by UV, Vis, or NIR pulses is broad and continuously growing. With this Review we present an overview of important experimental approaches, and aim to stimulate their further development and use. The respective pulse sequences where categorized by the purpose of the non-IR pulse either to create a particular probe process or to trigger the system under investigation. Our discussion focused on the information content of the spectra and the range of applications. An outlook in each subsection highlights challenges and potential developments of the presented experiments.

Multidimensional infrared spectroscopy is a technologically demanding discipline, which is strongly driven by technical development. This holds in particular for many of the mixed IR/non-IR experiments reviewed here. Important challenges still remain.

On the hardware side, there is a continuous drive for higher signal to noise ratios and shorter measurement times to make impossible experiments possible and to make challenging ones routine. New light sources are being developed that feature less noise, higher pulse repetition rates, higher pulse intensities, or ultrabroad bandwidths.[33,137–139] New approaches for detection and data acquisition are being devised to continuously improve data quality and access different observables.[25,87,140–144]

2D-IR spectra reveal many details of the molecular world and, accordingly, theoretical methods that aid interpretation of the spectra have to be very elaborate. This is even more so for the 2D spectroscopies discussed here, which, in addition to the requirements for regular 2D-IR spectroscopy, involve electronically excited states and strong excursions from equilibrium. Efforts for a theoretical description have to combine tools for an accurate description of the systems dynamics, for example, from molecular dynamics and calculation of electronic structure as well as efficient approaches to compute spectroscopic observables. Some of the experiments presented here offer great challenges to computational spectroscopy. Close collaborations between experimentalists and theoreticians are, therefore, required to advance our understanding of the sometimes complex spectra.

Another important challenge is to reduce experimental complexity to make the methods more and more accessible, both by reducing costs and by reducing the required technical know-how. As many of these experiments have been very challenging in the past, they have been used by only a few specialized research groups. However, hardware development continuously improves the ease of application through increased stability and automation,[25,144,145] which already has led to full-IR setups that can be handled by nonspecialists. Commercial 2D-IR spectrometers are becoming available,[145,146] which even allow the implementation of mixed pulse sequences. The range of scientists who can make use (direct or through cooperation with specialized groups) of the multidimensional experiments discussed here is, thus, expected to grow considerably in the near future.

Acknowledgements

We thank our co-workers and colleagues for their contributions, which are reflected in the list of references. We thank Thomas la Cour Jansen and Paul M. Donaldson for critically reading the manuscript. Kilian Fehre and Julian Schmidt-Engler are acknowledged for the German translation.

How to cite: *Angew. Chem. Int. Ed.* **2015**, *54*, 11624–11640
Angew. Chem. **2015**, *127*, 11790–11807

[1] K. Ataka, T. Kottke, J. Heberle, *Angew. Chem. Int. Ed.* **2010**, *49*, 5416–5424; *Angew. Chem.* **2010**, *122*, 5544–5553.
[2] E. A. Muller, B. Pollard, M. B. Raschke, *J. Phys. Chem. Lett.* **2015**, *6*, 1275–1284.
[3] S. Schlücker, *Angew. Chem. Int. Ed.* **2014**, *53*, 4756–4795; *Angew. Chem.* **2014**, *126*, 4852–4894.
[4] P. Hamm, M. T. Zanni, *Concepts and Methods of 2D Infrared Spectroscopy*, Cambridge University Press, Cambridge, **2011**.
[5] C. H. Londergan, C. P. Kubiak, *Chemistry* **2003**, *9*, 5962–5969.
[6] F.-W. Grevels, J. Jacke, W. E. Klotzbücher, C. Krüger, K. Seevogel, Y.-H. Tsay, *Angew. Chem. Int. Ed. Engl.* **1987**, *26*, 885–887; *Angew. Chem.* **1987**, *99*, 960–961.
[7] I. T. Suydam, C. D. Snow, V. S. Pande, S. G. Boxer, *Science* **2006**, *313*, 200–204.
[8] D. V. Kurochkin, S. R. G. Naraharisetty, I. V. Rubtsov, *Proc. Natl. Acad. Sci. USA* **2007**, *104*, 14209–14214.
[9] J. T. Sage, Y. Zhang, J. McGeehan, R. B. G. Ravelli, M. Weik, J. J. van Thor, *Biochim. Biophys. Acta Proteins Proteomics* **2011**, *1814*, 760–777.
[10] J. Manor, E. Arbely, A. Beerlink, M. Akkawi, I. T. Arkin, *J. Phys. Chem. Lett.* **2014**, *5*, 2573–2579.
[11] P. Hamm, M. Lim, R. M. Hochstrasser, *J. Phys. Chem. B* **1998**, *102*, 6123–6138.
[12] M. D. Fayer, *Annu. Rev. Phys. Chem.* **2009**, *60*, 21–38.
[13] P. Hamm, J. Helbing, J. Bredenbeck, *Annu. Rev. Phys. Chem.* **2008**, *59*, 291–317.
[14] N. T. Hunt, *Chem. Soc. Rev.* **2009**, *38*, 1837–1848.
[15] M. Khalil, N. Demirdöven, A. Tokmakoff, *J. Phys. Chem. A* **2003**, *107*, 5258–5279.

[16] M. Cho, *Two-dimensional Optical Spectroscopy*, CRC, Boca Raton, **2009**.
[17] S. Woutersen, P. Hamm, *J. Phys. Condens. Matter* **2002**, *14*, R1035.
[18] J. P. Ogilvie, K. J. Kubarych in *Advances In Atomic, Molecular, and Optical Physics*, Elsevier, Amsterdam, **2009**.
[19] W. Zhuang, T. Hayashi, S. Mukamel, *Angew. Chem. Int. Ed.* **2009**, *48*, 3750 – 3781; *Angew. Chem.* **2009**, *121*, 3804 – 3838.
[20] N.-H. Ge, M. T. Zanni, R. M. Hochstrasser, *J. Phys. Chem. A* **2002**, *106*, 962 – 972.
[21] M. Cho, *Chem. Rev.* **2008**, *108*, 1331 – 1418.
[22] J. Zheng, K. Kwak, M. D. Fayer, *Acc. Chem. Res.* **2007**, *40*, 75 – 83.
[23] Y. S. Kim, R. M. Hochstrasser, *J. Phys. Chem. B* **2009**, *113*, 8231 – 8251.
[24] H. Chen, H. Bian, J. Li, X. Wen, J. Zheng, *Int. Rev. Phys. Chem.* **2012**, *31*, 469 – 565.
[25] W. Rock, Y.-L. Li, P. Pagano, C. M. Cheatum, *J. Phys. Chem. A* **2013**, *117*, 6073 – 6083.
[26] I. V. Rubtsov, *Acc. Chem. Res.* **2009**, *42*, 1385 – 1394.
[27] J. C. Wright, *Annu. Rev. Phys. Chem.* **2011**, *62*, 209 – 230.
[28] M. C. Asplund, M. T. Zanni, R. M. Hochstrasser, *Proc. Natl. Acad. Sci. USA* **2000**, *97*, 8219 – 8224.
[29] L. P. Deflores, R. A. Nicodemus, A. Tokmakoff, *Opt. Lett.* **2007**, *32*, 2966.
[30] V. Cervetto, J. Helbing, J. Bredenbeck, P. Hamm, *J. Chem. Phys.* **2004**, *121*, 5935 – 5942.
[31] A. T. Messmer, K. M. Lippert, P. R. Schreiner, J. Bredenbeck, *Phys. Chem. Chem. Phys.* **2013**, *15*, 1509 – 1516.
[32] A. T. Messmer, K. M. Lippert, S. Steinwand, E.-B. W. Lerch, K. Hof, D. Ley, D. Gerbig, H. Hausmann, P. R. Schreiner, J. Bredenbeck, *Chem. Eur. J.* **2012**, *18*, 14989 – 14995.
[33] H. Bian, J. Li, X. Wen, Z. Sun, J. Song, W. Zhuang, J. Zheng, *J. Phys. Chem. A* **2011**, *115*, 3357 – 3365.
[34] S. Woutersen, P. Hamm, *J. Phys. Chem. B* **2000**, *104*, 11316 – 11320.
[35] S. Woutersen, Y. Mu, G. Stock, P. Hamm, *Proc. Natl. Acad. Sci. USA* **2001**, *98*, 11254 – 11258.
[36] T. L. C. Jansen, J. Knoester, *Biophys. J.* **2008**, *94*, 1818 – 1825.
[37] T. L. C. Jansen, J. Knoester, *Acc. Chem. Res.* **2009**, *42*, 1405 – 1411.
[38] H. M. Müller-Werkmeister, Y.-L. Li, E.-B. W. Lerch, D. Bigourd, J. Bredenbeck, *Angew. Chem. Int. Ed.* **2013**, *52*, 6214 – 6217; *Angew. Chem.* **2013**, *125*, 6334 – 6337.
[39] H. Chen, H. Bian, J. Li, X. Wen, Q. Zhang, W. Zhuang, J. Zheng, *J. Phys. Chem. B* **2015**, *119*, 4333 – 4349.
[40] H. Chen, H. Bian, J. Li, X. Wen, J. Zheng, *J. Phys. Chem. A* **2013**, *117*, 6052 – 6065.
[41] S. Woutersen, Y. Mu, G. Stock, P. Hamm, *Chem. Phys.* **2001**, *266*, 137 – 147.
[42] J. Zheng, K. Kwak, J. Xie, M. D. Fayer, *Science* **2006**, *313*, 1951 – 1955.
[43] J. Zheng, K. Kwak, J. Asbury, X. Chen, I. R. Piletic, M. D. Fayer, *Science* **2005**, *309*, 1338 – 1343.
[44] J. Zheng, K. Kwak, J. Xie, M. D. Fayer, *Science* **2006**, *313*, 1951 – 1955.
[45] J. F. Cahoon, K. R. Sawyer, J. P. Schlegel, C. B. Harris, *Science* **2008**, *319*, 1820 – 1823.
[46] N. Demirdöven, M. Khalil, A. Tokmakoff, *Phys. Rev. Lett.* **2002**, *89*, 237401.
[47] M. T. Zanni, M. C. Asplund, R. M. Hochstrasser, *J. Chem. Phys.* **2001**, *114*, 4579.
[48] S. T. Roberts, J. J. Loparo, A. Tokmakoff, *J. Chem. Phys.* **2006**, *125*, 084502.
[49] K. Kwak, S. Park, I. J. Finkelstein, M. D. Fayer, *J. Chem. Phys.* **2007**, *127*, 124503.
[50] L. J. G. W. van Wilderen, D. Kern-Michler, H. M. Müller-Werkmeister, J. Bredenbeck, *Phys. Chem. Chem. Phys.* **2014**, *16*, 19643 – 19653.
[51] D. G. Kuroda, J. D. Bauman, J. R. Challa, D. Patel, T. Troxler, K. Das, E. Arnold, R. M. Hochstrasser, *Nat. Chem.* **2013**, *5*, 174 – 181.
[52] J. K. Chung, M. C. Thielges, M. D. Fayer, *J. Am. Chem. Soc.* **2012**, *134*, 12118 – 12124.
[53] K. Kwac, M. Cho, *J. Chem. Phys.* **2003**, *119*, 2256.
[54] Z. Ren, A. S. Ivanova, D. Couchot-Vore, S. Garrett-Roe, *J. Phys. Chem. Lett.* **2014**, *5*, 1541 – 1546.
[55] J. D. Eaves, J. J. Loparo, C. J. Fecko, S. T. Roberts, A. Tokmakoff, P. L. Geissler, *Proc. Natl. Acad. Sci. USA* **2005**, *102*, 13019 – 13022.
[56] D. Kraemer, M. L. Cowan, A. Paarmann, N. Huse, E. Nibbering, T. Elsaesser, R. J. D. Miller, *Proc. Natl. Acad. Sci. USA* **2008**, *105*, 437 – 442.
[57] T. L. C. Jansen, B. M. Auer, M. Yang, J. L. Skinner, *J. Chem. Phys.* **2010**, *132*, 224503.
[58] J. Bredenbeck, J. Helbing, R. Behrendt, C. Renner, L. Moroder, J. Wachtveitl, P. Hamm, *J. Phys. Chem. B* **2003**, *107*, 8654 – 8660.
[59] L. J. G. W. van Wilderen, A. T. Messmer, J. Bredenbeck, *Angew. Chem. Int. Ed.* **2014**, *53*, 2667 – 2672; *Angew. Chem.* **2014**, *126*, 2705 – 2710.
[60] E. R. Andresen, P. Hamm, *J. Phys. Chem. B* **2009**, *113*, 6520 – 6527.
[61] V. Cervetto, P. Hamm, J. Helbing, *J. Phys. Chem. B* **2008**, *112*, 8398 – 8405.
[62] J. Bredenbeck, J. Helbing, A. Sieg, T. Schrader, W. Zinth, C. Renner, R. Behrendt, L. Moroder, J. Wachtveitl, P. Hamm, *Proc. Natl. Acad. Sci. USA* **2003**, *100*, 6452 – 6457.
[63] C. Kolano, J. Helbing, M. Kozinski, W. Sander, P. Hamm, *Nature* **2006**, *444*, 469 – 472.
[64] M. J. Tucker, M. Abdo, J. R. Courter, J. Chen, S. P. Brown, A. B. Smith, R. M. Hochstrasser, *Proc. Natl. Acad. Sci. USA* **2013**, *110*, 17314 – 17319.
[65] H. S. Chung, Z. Ganim, K. C. Jones, A. Tokmakoff, *Proc. Natl. Acad. Sci. USA* **2007**, *104*, 14237 – 14242.
[66] C. R. Baiz, Y.-S. Lin, C. S. Peng, K. A. Beauchamp, V. A. Voelz, V. S. Pande, A. Tokmakoff, *Biophys. J.* **2014**, *106*, 1359 – 1370.
[67] C. S. Peng, C. R. Baiz, A. Tokmakoff, *Proc. Natl. Acad. Sci. USA* **2013**, *110*, 9243 – 9248.
[68] M. Delor, I. V. Sazanovich, M. Towrie, S. J. Spall, T. Keane, A. J. Blake, C. Wilson, A. J. H. M. Meijer, J. A. Weinstein, *J. Phys. Chem. B* **2014**, *118*, 11781 – 11791.
[69] L. M. Kiefer, J. T. King, K. J. Kubarych, *J. Phys. Chem. A* **2014**, *118*, 9853 – 9860.
[70] R. Kania, A. I. Stewart, I. P. Clark, G. M. Greetham, A. W. Parker, M. Towrie, N. T. Hunt, *Phys. Chem. Chem. Phys.* **2010**, *12*, 1051 – 1063.
[71] M. S. Lynch, K. M. Slenkamp, M. Khalil, *J. Chem. Phys.* **2012**, *136*, 241101.
[72] M. S. Lynch, K. M. Slenkamp, M. Cheng, M. Khalil, *J. Phys. Chem. A* **2012**, *116*, 7023 – 7032.
[73] A. I. Stewart, J. A. Wright, G. M. Greetham, S. Kaziannis, S. Santabarbara, M. Towrie, A. W. Parker, C. J. Pickett, N. T. Hunt, *Inorg. Chem.* **2010**, *49*, 9563 – 9573.
[74] C. R. Baiz, R. McCanne, K. J. Kubarych, *J. Am. Chem. Soc.* **2009**, *131*, 13590 – 13591.
[75] M. Delor, P. A. Scattergood, I. V. Sazanovich, A. W. Parker, G. M. Greetham, A. J. H. M. Meijer, M. Towrie, J. A. Weinstein, *Science* **2014**, *346*, 1492 – 1495.
[76] Y. Yue, T. A. Grusenmeyer, Z. Ma, P. Zhang, R. Schmehl, D. N. Beratan, I. V. Rubtsov, *Dalton Trans.* **2015**, *44*, 8609 – 8616.
[77] C. Dumont, T. Emilsson, M. Gruebele, *Nat. Methods* **2009**, *6*, 515 – 519.

[78] D. S. Pearson, G. Holtermann, P. Ellison, C. Cremo, M. A. Geeves, *Biochem. J.* **2002**, *366*, 643 – 651.
[79] M. Gutman, E. Nachliel, *Biochim. Biophys. Acta* **1990**, *1015*, 391 – 414.
[80] J. S. Huebner, A. E. Popp, K. R. Williams, *J. Chem. Educ.* **1988**, *65*, 102.
[81] H. Fabian, D. Naumann, *Methods* **2004**, *34*, 28 – 40.
[82] J. Bredenbeck, J. Helbing, P. Hamm, *Rev. Sci. Instrum.* **2004**, *75*, 4462.
[83] P. Bodis, M. R. Panman, B. H. Bakker, A. Mateo-Alonso, M. Prato, W. J. Buma, A. M. Brouwer, E. R. Kay, D. A. Leigh, S. Woutersen, *Acc. Chem. Res.* **2009**, *42*, 1462 – 1469.
[84] D. Strasfeld, S.-H. Shim, M. T. Zanni, *Phys. Rev. Lett.* **2007**, *99*, 038102.
[85] J. Bredenbeck, J. Helbing, P. Hamm, *J. Am. Chem. Soc.* **2004**, *126*, 990 – 991.
[86] J. Bredenbeck, J. Helbing, K. Nienhaus, G. U. Nienhaus, P. Hamm, *Proc. Natl. Acad. Sci. USA* **2007**, *104*, 14243 – 14248.
[87] C. R. Baiz, M. J. Nee, R. McCanne, K. J. Kubarych, *Opt. Lett.* **2008**, *33*, 2533.
[88] R. R. Ernst, G. Bodenhausen, A. Wokaun, *Principles of Nuclear Magnetic Resonance in One and Two Dimensions*, Clarendon, Oxford, **1997**.
[89] J. Schleucher, B. Schwoerer, R. K. Thauer, C. Griesinger, *J. Am. Chem. Soc.* **1995**, *117*, 2941 – 2942.
[90] W. Xiong, J. E. Laaser, P. Paoprasert, R. A. Franking, R. J. Hamers, P. Gopalan, M. T. Zanni, *J. Am. Chem. Soc.* **2009**, *131*, 18040 – 18041.
[91] S. Ruetzel, M. Kullmann, J. Buback, P. Nuernberger, T. Brixner, *Phys. Rev. Lett.* **2013**, *110*, 148305.
[92] L. K. Iwaki, D. D. Dlott, *J. Phys. Chem. A* **2000**, *104*, 9101 – 9112.
[93] D. D. Dlott, *Chem. Phys.* **2001**, *266*, 149 – 166.
[94] A. Laubereau, W. Kaiser, *Rev. Mod. Phys.* **1978**, *50*, 607 – 665.
[95] Y. Sun, B. C. Pein, D. D. Dlott, *J. Phys. Chem. B* **2013**, *117*, 15444 – 15451.
[96] Z. Wang, A. V. Pakoulev, D. D. Dlott, *Science* **2002**, *296*, 2201 – 2203.
[97] J. C. Deàk, Y. Pang, T. D. Sechler, Z. Wang, D. D. Dlott, *Science* **2004**, *306*, 473 – 476.
[98] J. C. Deàk, S. T. Rhea, L. K. Iwaki, D. D. Dlott, *J. Phys. Chem. A* **2000**, *104*, 4866 – 4875.
[99] V. Kozich, Ł. Szyc, E. Nibbering, W. Werncke, T. Elsaesser, *Chem. Phys. Lett.* **2009**, *473*, 171 – 175.
[100] B. C. Pein, D. D. Dlott, *J. Phys. Chem. A* **2014**, *118*, 965 – 973.
[101] B. C. Pein, Y. Sun, D. D. Dlott, *J. Phys. Chem. B* **2013**, *117*, 10898 – 10904.
[102] F. Fournier, R. Guo, E. M. Gardner, P. M. Donaldson, C. Loeffeld, I. R. Gould, K. R. Willison, D. R. Klug, *Acc. Chem. Res.* **2009**, *42*, 1322 – 1331.
[103] W. Zhao, J. C. Wright, *Phys. Rev. Lett.* **2000**, *84*, 1411 – 1414.
[104] W. Zhao, J. C. Wright, *Phys. Rev. Lett.* **1999**, *83*, 1950 – 1953.
[105] P. M. Donaldson, R. Guo, F. Fournier, E. M. Gardner, L. M. C. Barter, C. J. Barnett, I. R. Gould, D. R. Klug, D. J. Palmer, K. R. Willison, *J. Chem. Phys.* **2007**, *127*, 114513.
[106] R. Guo, F. Fournier, P. M. Donaldson, E. M. Gardner, I. R. Gould, D. R. Klug, *Phys. Chem. Chem. Phys.* **2009**, *11*, 8417 – 8421.
[107] R. Guo, S. Mukamel, D. R. Klug, *Phys. Chem. Chem. Phys.* **2012**, *14*, 14023 – 14033.
[108] F. Fournier, E. M. Gardner, R. Guo, P. M. Donaldson, L. M. C. Barter, D. J. Palmer, C. J. Barnett, K. R. Willison, I. R. Gould, D. R. Klug, *Anal. Biochem.* **2008**, *374*, 358 – 365.
[109] R. Guo, M. Miele, E. M. Gardner, F. Fournier, K. M. Kornau, I. R. Gould, D. R. Klug, *Faraday Discuss.* **2011**, *150*, 161 – 174; discussion R. Guo, M. Miele, E. M. Gardner, F. Fournier, K. M. Kornau, I. R. Gould, D. R. Klug, *Faraday Discuss.* **2011**, *150*, 257 – 292.
[110] L. R. Valim, J. A. Davies, K. T. Jensen, R. Guo, K. R. Willison, C. M. Spickett, A. R. Pitt, D. R. Klug, *J. Phys. Chem. B* **2014**, *118*, 12855 – 12864.
[111] E. S. Boyle, N. A. Neff-Mallon, J. C. Wright, *J. Phys. Chem. A* **2013**, *117*, 12401 – 12408.
[112] J. Bredenbeck, A. Ghosh, M. Smits, M. Bonn, *J. Am. Chem. Soc.* **2008**, *130*, 2152 – 2153.
[113] C. Hess, M. Cho, M. Bonn, *Surf. Sci.* **2002**, *502*, 123 – 128.
[114] J. H. Hunt, P. Guyot-Sionnest, Y. R. Shen, *Chem. Phys. Lett.* **1987**, *133*, 189 – 192.
[115] R. E. Pool, J. Versluis, E. H. G. Backus, M. Bonn, *J. Phys. Chem. B* **2011**, *115*, 15362 – 15369.
[116] M. J. Nee, R. McCanne, K. J. Kubarych, M. Joffre, *Opt. Lett.* **2007**, *32*, 713.
[117] J. Bredenbeck, A. Ghosh, H.-K. Nienhuys, M. Bonn, *Acc. Chem. Res.* **2009**, *42*, 1332 – 1342.
[118] W. Xiong, J. E. Laaser, R. D. Mehlenbacher, M. T. Zanni, *Proc. Natl. Acad. Sci. USA* **2011**, *108*, 20902 – 20907.
[119] Z. Zhang, L. Piatkowski, H. J. Bakker, M. Bonn, *Nat. Chem.* **2011**, *3*, 888 – 893.
[120] P. C. Singh, S. Nihonyanagi, S. Yamaguchi, T. Tahara, *J. Chem. Phys.* **2013**, *139*, 161101.
[121] H. Bian, J. Li, H. Chen, K. Yuan, X. Wen, Y. Li, Z. Sun, J. Zheng, *J. Phys. Chem. C* **2012**, *116*, 7913 – 7924.
[122] P. M. Donaldson, P. Hamm, *Angew. Chem. Int. Ed.* **2013**, *52*, 634 – 638; *Angew. Chem.* **2013**, *125*, 662 – 666.
[123] J. Nishida, C. Yan, M. D. Fayer, *J. Phys. Chem. C* **2014**, *118*, 523 – 532.
[124] D. G. Osborne, J. A. Dunbar, J. G. Lapping, A. M. White, K. J. Kubarych, *J. Phys. Chem. B* **2013**, *117*, 15407 – 15414.
[125] D. E. Rosenfeld, Z. Gengeliczki, B. J. Smith, T. D. P. Stack, M. D. Fayer, *Science* **2011**, *334*, 634 – 639.
[126] C.-S. Hsieh, M. Okuno, J. Hunger, E. H. G. Backus, Y. Nagata, M. Bonn, *Angew. Chem. Int. Ed.* **2014**, *53*, 8146 – 8149; *Angew. Chem.* **2014**, *126*, 8284 – 8288.
[127] Z. Zhang, L. Piatkowski, H. J. Bakker, M. Bonn, *J. Chem. Phys.* **2011**, *135*, 021101.
[128] J. E. Laaser, M. T. Zanni, *J. Phys. Chem. A* **2013**, *117*, 5875 – 5890.
[129] C. Liang, T. L. C. Jansen, *J. Phys. Chem. B* **2013**, *117*, 6937 – 6945.
[130] C. Liang, M. Louhivuori, S. J. Marrink, T. L. C. Jansen, J. Knoester, *J. Phys. Chem. Lett.* **2013**, *4*, 448 – 452.
[131] J. K. Carr, L. Wang, S. Roy, J. L. Skinner, *J. Phys. Chem. B* **2015**, *119*, 8969 – 8983.
[132] S. Nihonyanagi, S. Yamaguchi, T. Tahara, *J. Chem. Phys.* **2009**, *130*, 204704.
[133] M. Yeganeh, S. Dougal, H. Pink, *Phys. Rev. Lett.* **1999**, *83*, 1179 – 1182.
[134] J. E. Laaser, D. R. Skoff, J.-J. Ho, Y. Joo, A. L. Serrano, J. D. Steinkruger, P. Gopalan, S. H. Gellman, M. T. Zanni, *J. Am. Chem. Soc.* **2014**, *136*, 956 – 962.
[135] A. Ghosh, J.-J. Ho, A. L. Serrano, D. R. Skoff, T. Zhang, M. T. Zanni, *Faraday Discuss.* **2015**, *177*, 493 – 505.
[136] M. Smits, A. Ghosh, J. Bredenbeck, S. Yamamoto, M. Müller, M. Bonn, *New J. Phys.* **2007**, *9*, 390 – 409.
[137] J. Biegert, P. K. Bates, O. Chalus, *IEEE J. Sel. Top. Quantum Electron.* **2012**, *18*, 531 – 540.
[138] P. B. Petersen, A. Tokmakoff, *Opt. Lett.* **2010**, *35*, 1962 – 1964.
[139] C. Calabrese, A. M. Stingel, L. Shen, P. B. Petersen, *Opt. Lett.* **2012**, *37*, 2265 – 2267.
[140] S.-H. Shim, M. T. Zanni, *Phys. Chem. Chem. Phys.* **2009**, *11*, 748 – 761.
[141] J. Helbing, P. Hamm, *J. Opt. Soc. Am. B* **2011**, *28*, 171.

[142] P. M. Donaldson, H. Strzalka, P. Hamm, *Opt. Express* **2012**, *20*, 12761 – 12770.
[143] J. Réhault, M. Maiuri, C. Manzoni, D. Brida, J. Helbing, G. Cerullo, *Opt. Express* **2014**, *22*, 9063 – 9072.
[144] J. D. Leger, C. M. Nyby, C. Varner, J. Tang, N. I. Rubtsova, Y. Yue, V. V. Kireev, V. D. Burtsev, L. N. Qasim, G. I. Rubtsov, et al., *Rev. Sci. Instrum.* **2014**, *85*, 083109.
[145] D. R. Skoff, J. E. Laaser, S. S. Mukherjee, C. T. Middleton, M. T. Zanni, *Chem. Phys.* **2013**, *422*, 8 – 15.
[146] M. T. Zanni, C. T. Middleton, M. Arrigoni, J. Henrich, *Laser Focus World* **2013**.

Received: April 6, 2015
Published online: August 26, 2015